Body-Coupled Monopole UWB Antenna for Wearable Medical Microwave Imaging Applications

Body-Coupled Monopole UWB Antenna for Wearable Medical Microwave Imaging Applications

F. Wang[1] T. Arslan[2]

Abstract – **This paper presents a body-coupled ultra-wideband (UWB) antenna configuration for near-field microwave imaging applications. An UWB antenna is designed for wearable applications that will be require direct contract with the human body. In order to optimize antenna size and near-field radiation characteristics, to match the underlying body tissue, a stretchable dielectric spacer (a mixture of polydimethylsiloxane (PDMS) and Ecoflex) was placed between the designed antenna and a human phantom. The size of the proposed body-coupled antenna configuration is around 0.15λ×0.15λ at the lowest operational frequency of 2GHz. The variation effects of the dielectric spacer on body matching performance with the designed UWB antenna placed on a voxel-based phantom is investigated in the frequency range 0.1-12GHz across sagittal cuts.**

1 INTRODUCTION

Microwave Imaging (MWI) has been promoted as an alternative medical imaging technique. It operates by transmitting a microwave impulse signal into the interested human tissue section and receiving the scatted signals to generate maps of the electrical property distribution [1]. MWI has addressed different medical applications such as early-stage breast tumor, brain tumor, brain-stroke and lung tumor detection and imaging [2]. Recently, wearable ultra-wideband (UWB) monopole antennas were suggested for long-term breast cancer detection. However, the antenna coupling is a challenge for microwave imaging applications especially for near-filed imaging as the antenna is in contact with biological tissues that will have very different propagation behavior compared to free space. This is because of nearfield body coupling [3].

In [4], a dielectric spacer with low loss and permittivity matching the skin tissue was added under a body-worn antenna. This is to allow the release of more energy into the body and reduce the antenna sensitivity. Furthermore, investigations are carried out to show that the dielectric spacer allows less microwave signal loss and reduce the body surface reflection. Meanwhile, the minimization of the UWB antenna with lower operating frequency could be achieved by using different dielectric spacers matching different human tissues [5]. A dielectric spacer with adjustable permittivity and low loss can be achieved by using a mixture of PDMS and Ecoflex and other materials. Moreover, the combination of PDMS and Ecoflex are flexible, low-cost and relatively isotropic for wearable applications [6]. In this paper, a flexible dielectric spacer is added to a wearable UWB antenna design to minimize the size and improve body-coupling performance.

The paper is organized as follows: section 2 presents the proposed small monopole UWB antenna with PDMS/Ecoflex-based dielectric spacer for radar-based microwave imaging. In the same section, we describe simulations that are carried out to design the proposed UWB antenna with adjustable dielectric spacer by mixing PDMS and other material for a voxel-based human phantom. Section 3 demonstrates the effect of variation of the different dielectric spacers mounted on the antenna on reflection coefficient. Finally, a brief conclusion is given section 4.

2 PROPOSED BODY-COUPED ANTENNA

2.1 Monopole UWB antenna design

In this design, a single-side monopole antenna is chosen for UWB radar-based microwave imaging applications. A 50Ω coplanar waveguide (CPW) line is designed (with 3mm wide feeding line and 0.3mm gap between feeding line and ground) to feed the proposed antenna. A vertical sub-miniature Version A (SMA) connector is selected for practical applications. In Figure 1, the antenna is fabricated on RO4350 substrate with permittivity (ϵ_r=3.66) and 0.508 mm thickness with size of 17.8×18.2 mm^2.

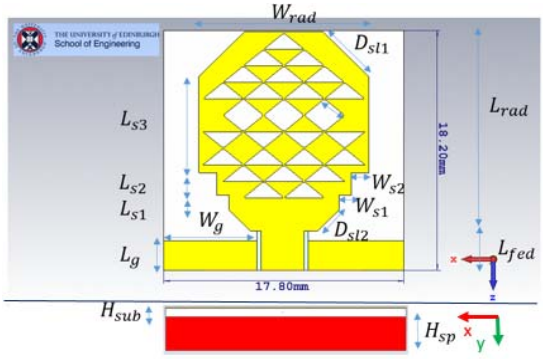

Figure 1: Geometry of the proposed body-coupled UWB Antenna.

In order to decrease the effect of clutter on the image and reduce the number of imaging artefacts, more sensing antennas with less footprint are mounted on the small interested tissue area [7]. The size of antenna was reduced by using multi-step staircase and fractal slots on the radiator by increasing the electrical length of the radiator [8]. Each dimension is listed in Table. 1.

[1] Institute for Integrated Micro and Nano Systems School of Engineering, University of Edinburgh Edinburgh, Unite Kingdom, e-mail: f.wang@ed.ac.uk, tel.: +44 07526700154.
[2] Institute for Integrated Micro and Nano Systems School of Engineering, University of Edinburgh Edinburgh, Unite Kingdom, e-mail: T.Arslan@ed.ac.uk, tel.: +44 0131 6505592

W_{rad}	5.8mm	L_{s1}	1.1 mm
L_{rad}	15.2 mm	L_{s2}	1.7 mm
L_{fed}	3 mm	L_{s3}	7.3 mm
D_{sl1}	4.8 mm	W_g	6.9 mm
D_{sl2}	2.1 mm	L_g	2.25 mm
W_{s1}	0.9 mm	H_{sub}	2 mm
W_{s2}	1.3 mm	H_{sp}	0.508 mm

Table 1: Dimension of the body-coupled antenna.

Further size reduction can be achieved by using a high permittivity and low loss dielectric spacer as shown in Figure 2. This will reduce the near-field loading and increase energy release into the body. The spacer need to be kept to minimum footprint to enhance diagnosis accuracy of the imaging through allowing the use of more sensing elements. Further discussion on spacer dimensions is presented in Section III. In this design, a potential solution using the soft mixture (i.e. PDMS and Excoflex) spacer (providing different dielectrics constant values, through different mixture combinations, within the same antenna substrate size and a thickness of 2 mm) is placed between the proposed antenna and the human phantom. The performance of the proposed antenna is evaluated in Computer Simulation Technology Microwave Studio (CST MWS) below.

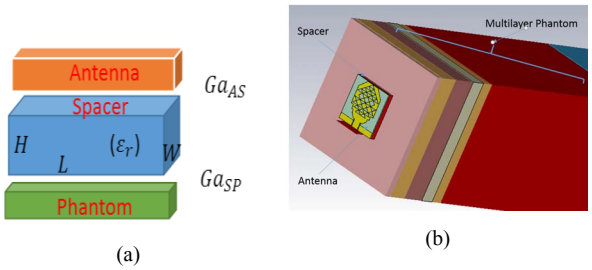

(a) (b)

Figure 3: Configuration of antenna with dielectric spacer mounted on human phantom (a) Structure of antenna elements (b) Antenna with spacer mounted on planar model in CST MWS

2.2 Simulated Results

Three scenarios are chosen for studying the return loss (S_{11}) of the proposed configuration of the body-coupled UWB antenna: Frist, the designed UWB antenna is placed in free space without a spacer. Second, the designed antenna is placed at the front of the chest for a heterogeneous human phantom Ella [9]. Third, the designed antenna and the spacer with dielectric constant (ε_r) of 37 is placed at the same positon in the second scenario. The voxel-based phantom was used with the dielectric properties of the tissues associated with the phantom were assigned, ranging from 0.1 GHz to 10 GHz. In Figure 3, the proposed body-coupled antenna was placed at the front of the chest for the body phantom.

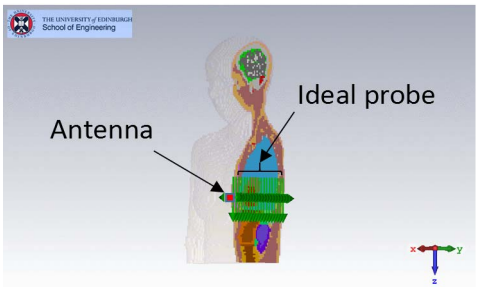

Figure 3: The body-coupled Antenna mounted on human phantom (Ella) for the simulation.

As the antenna is placed on the front of the chest, S_{11} is mainly influenced by signal reflection from the skin tissue on the chest, due to high dielectric constant value. According to [5], the dielectric constant of skin is around 37. To achieve good ability to efficiently couple power to human tissue, the dielectrics constant (ε_r) of the dielectric spacer is configured as 37 with low loss (i.e. 0.002) in the following simulation. This will be fabricated with different percentages of PDMS and Excoflex. In Figure. 3, several ideal probes are inserted in different depths from the phantom surface to measure scattered signal in different positions over the frequency range from 0.1 GHz to 12 GHz.

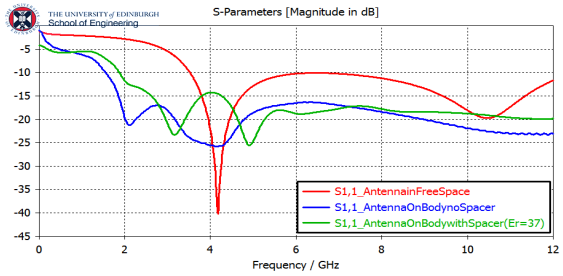

Figure 4: Simulation of the proposed antenna with spacer in free space and over a human phantom(Ella)

Figure. 4. shows the presence of the human tissue shifts the lower cutoff frequency of the designed antenna from 3.8 GHz (free space scenario) to a lower frequency (i.e.1.9 GHz, when only the antenna is placed on the phantom, and 2.5 GHz when antenna is mounted on a spacer (with ϵ_r= 37) placed on the phantom).

Furthermore, stimulation is performed with a Gaussian pulse defined in the frequency range from 0 GHz to 12 GHz in time-domain. The received signals from the placed probes have expected time delays due to the signals going through different depths

within the human phantom. Meanwhile, these results show that the dielectric spacers could increase the release of energy to the different mounted tissues as shown in Figure 5.

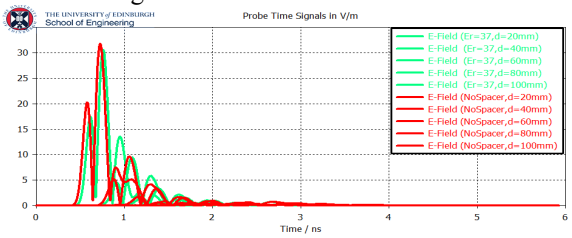

Figure 5: Received probe signals under simulation setup in Figure.3

Figure 6 illustrates a difference in the received when the probe is inserted deeper within tissue (60 mm from phantom surface). There is a time delay between the received signals with and without the spacer. The time delay is proportional to the thickness of the spacer. Higher signal level is detected by the probe since the dielectric spacer extends the impedance matching over a larger frequency range which allows more energy to travel deeper into tissue.

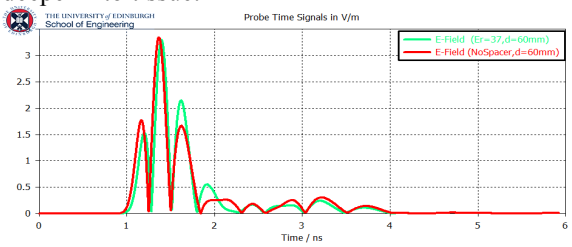

Figure 6: Received probe signals at 60mm away from phantom surface

3 EFFECT ON DIRELECTRIC SPACERS

In this section, various simulations were done to study the variation effect of the dielectric spacer such as the difference of dielectric constant (ε_r), the dimensions ($W \times L \times H$), and air-gaps between other elements (Ga_{AS} is the gap between antenna and spacer, and Ga_{SP} is the gap between spacer and phantom) on the return loss (S_{11}) of the proposed body-coupled antenna configuration when it was placed on the mentioned voxel-based phantom as shown in Figure 3.

3.1 Effect of dielectric constant

In Figure 7, the variations of the spacer dielectric constant (ε_r) has a small effect on the reflection coefficient (S_{11}) at lower frequencies around 2 GHz. The best matching exits when ε_r equals to 60. The major effect of ε_r exits when the antenna operates at high frequency ranges and a higher ε_r leads to a better body matching performance of the antenna.

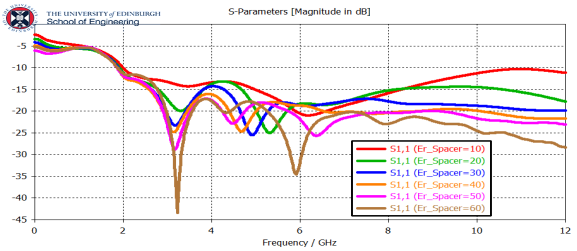

Figure 7: Simulated reflection coefficient with spacers with different dielectric constants

3.2 Effect of dimension of dielectric spacers

In Figure 8, the larger spacer helps achieve lower cutoff frequency as the size ($W \times L$) increases in horizontal direction (x-axis and y-axis). The tradeoff is a larger space taken and more footprint on the limited area of human body for wearable applications.

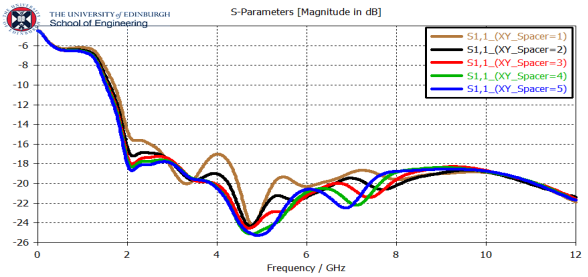

Figure 8: Simulated reflection coefficient with spacers with different extension lengths

Figure 9 shows that the lower cutoff frequency shifts to a higher frequency as the thickness of spacers increase. Thus, the thickness of the spacer causes an unstable oscillation of S_{11}. Besides, the ringing phenomenon happens over the frequency due to the microwave signal oscillating from the excited resonant mode when the signal goes through the spacer. In this case, the minimum ringing amplitude and largest bandwidth is achieved when the extension of the thickness is 1 mm.

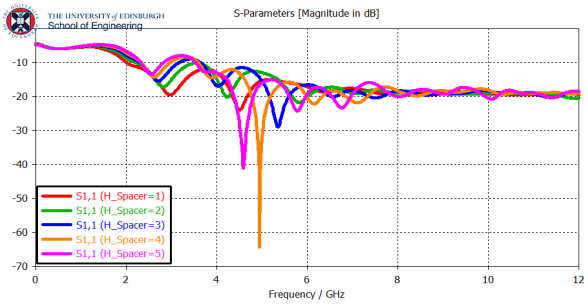

Figure 9: Simulated reflection coefficient with spacers with different extension of spacer size

3.2 Effect of air-gaps

In Figures 10-11, the air gaps have significant effect on the body matching performance over the operating frequency. In addition, the air gap between spacer and phantom (Ga_{SP}) has more distortion than the air gap between antenna and spacer (Ga_{AS}).

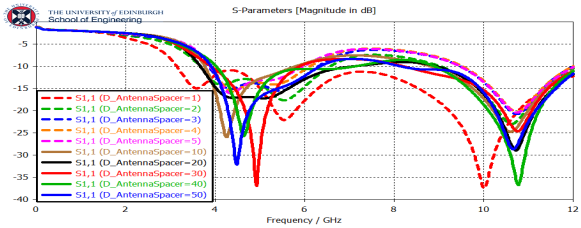

Figure 10: Simulated reflection coefficient with different Ga_{AS}

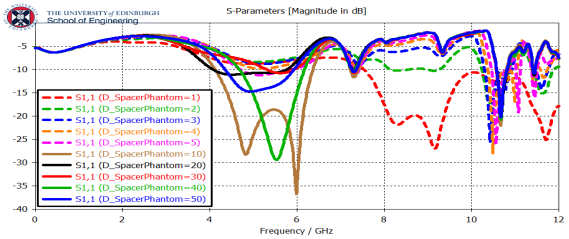

Figure 11: Simulated reflection coefficient with different Ga_{SP}

In the high operating frequency range, the proposed antenna is more sensitive to the air gaps where the higher cut-off frequency shifts to lower frequency. In the low operating frequency range, the lower cut-off frequency shifts to lower frequency as each element approaches other elements. In another word, the body effect has propagation with the distance between antenna, phantom and spacer. Furthermore, the dot lines show that the propagation relationship between each element only exits within a short range, and then suddenly changes when the gaps is larger than the quarter wavelength (30 mm) of the lowest operating frequency (2.5 GHz) as shown with the solid lines.

4 Conclusion

This paper presents a potentially stretchable solution using a mixture of PDMS and Excoflex for a body-coupled UWB antenna for wearable applications. This is difficult to achieve using traditional methods using planar and nonflexible dielectric spacers. Ours results demonstrate that the dielectric constant of the spacer has positive effect on the impedance matching of the proposed antenna. Best matching is achieved when the dielectric constant is close to the underlying tissue. The cross-section size of the dielectric spacer is minimized to the same size as the antenna substrate. Due to the stretchable property of the proposed body-coupled antenna, it can obtain lower cut-off frequency when the cross-section size of the dielectric spacer increases. The thickness of the dielectric spacer is chosen based on the center the operational frequency and is equal to 3mm in this design to achieve coupling to the chest. Furthermore, air-gaps can be avoided using this stretchable solution eliminating their negative effect on antenna performance.

References

[1] W. Shao, A. Edalati, T. R. McCollough, and W. J. McCollough, "A Phase Confocal Method for Near-Field Microwave Imaging," IEEE Transactions on Microwave Theory and Techniques, 2017.

[2] R. Chandra, H. Zhou, I. Balasingham, and R. M. Narayanan, "On the opportunities and challenges in microwave medical sensing and imaging," IEEE Transactions on Biomedical Engineering, vol. 62, pp. 1667-1682, 2015.

[3] K. G. Kjelgård and T. S. Lande, "Body coupled wideband monopole antenna," in Antennas & Propagation Conference (LAPC), 2016 Loughborough, pp. 1-5, 2016.

[4] F. Merli, B. Fuchs, J. R. Mosig, and A. K. Skrivervik, "The effect of insulating layers on the performance of implanted antennas," IEEE Transactions on Antennas and Propagation, vol. 59, pp. 21-31, 2011.

[5] K. G. Kjelgård and T. S. Lande, "Body-coupled, wideband antennas," in Biomedical Circuits and Systems Conference (BioCAS), 2015 IEEE, 2015.

[6] J. Trajkovikj, J. F. Zurcher, and A. K. Skrivervik, "Soft and flexible antennas on permittivity adjustable PDMS substrates," in Antennas and Propagation Conference (LAPC), Loughborough, pp. 1-4, 2012.

[7] M. Ahadi, M. B. M. Isa, M. I. B. Saripan, and W. Z. W. Hasan, "Square monopole antenna for microwave imaging, design and characterisation," IET Microwaves, Antennas & Propagation, vol. 9, pp. 49-57, 2015.

[8] F. Wang and T. Arslan, "Inkjet-printed antenna on flexible substrate for wearable microwave imaging applications," Antennas & Propagation Conference (LAPC), 2016 Loughborough, 2016.

[9] S. Koulouridis, G. Kiziltas, Y. Zhou, D. J. Hansford, and J. L. Volakis, "Polymer–ceramic composites for microwave applications: fabrication and performance assessment," IEEE Transactions on Microwave Theory and Techniques, vol. 54, pp. 4202-4208, 2006.